International Journal of Bio-Science and Bio-Technology
Vol.7, No.5 (2015), pp.247-258
http://dx.doi.org/10.14257/ijbsbt.2015.7.5.23

# Determination of Equivalent Dose of Specific Organs in Computational Age Dependent Phantoms using Proton Therapy in Geant4

*S.N.L Sirisha and Sonali Bhatnagar*

*Department of Physics and Computer Science*
*Dayalbagh Educational Institute*
*Dayalbagh, Agra-282005*
*deisonali.bhatnagar@gmail.com*

***Abstract***

*The paper is in continuation of the previous work in which the effect on Bragg peak position, range and penumbra width of proton beam in radiation therapy is observed when inhomogenities such as brain, kidney and thyroid are placed in a homogeneous medium. The human organs along with the positioning of the tumour region were designed and the suitable energy range for each tumour of the human organ was optimized. A significant shift in the Bragg peak position was observed in each case i.e., approx. -0.36% for muscular skeleton, -0.44% for soft tissue (S. Bhatnagar et.al, 2014) [1]. In this paper, we will discuss the significant effect of the absorbed dose of proton beam during treatment in different ages. Distinct phantom volumes with their respective organs i.e. brain, kidney and thyroid of children at various ages such as 0, 1, 5, 10, 15 years and also an adult are considered from OAK RIDGE NATIONAL LABORATORY (ORNL) report (M. Cristy et.al) [2] for present simulation study. The relation between dose equivalent, absorbed dose as function of depth to target volume is computed. We observed that the dose deposition is dependent on the age where patient at younger age receives dose at higher rate while it gradually decreases in the other cases i.e. 10 year, 15 year and adult. The step length of the particle is varied which imposes a limit during particle interaction in the medium per unit length. The obtained dose rate on varying the step length is compared among the Geant4 9.3 and 9.4 versions to observe its data accuracy.*

***Key Words:*** *Proton therapy, Absorbed Dose, Dose Equivalent, Geant4, Step length*

## 1. Introduction

The inhomogeneous medium plays an important role in effecting stopping power and range of proton beam during treatment. We have studied the effect on Bragg peak and its parameters in case of curing tumours in a 15 year teenager (*S. Bhatnagar et.al, 2014*) [1] for different regions i.e. brain, kidney and thyroid. As extension of this work, we compute the absorbed dose and dose equivalent of proton beam in curing brain, kidney and thyroid tumour at different ages of phantom i.e. a new born baby (0 year), 1 year, $10^{th}$, 15 year children and an adult are considered for the study. The effect on production of soft electrons, photons and particle traversing dose distribution of proton beam are studied on varying step size of the particle. The accuracy of the data was observed on comparing the versions Geant4.9.3 and 9.4.

Proton therapy is developed for providing an improved treatment compared to Intensity modulated radiotherapy and other photon techniques. Protons are mainly used for curing head neck, ocular, breast and paediatric tumours (*Wilson et.al, 2005*) [3]. Due to the finite range of protons, they can deposit maximum energy at a depth in Bragg Peak for the

ISSN: 2233-7849 IJBSBT

treatment of deep seated tumours while sparing the healthy tissues surrounding it. The proton trajectories are controlled by magnetic field. The range of proton beam is dependent on primary energy and physical characteristics of the target material (*Stephen J. Dowdell et.al, 2011*) [18]. The ionisation density of proton increases with increased depth, leading to the deposition of the majority of the energy at depth, inside the target. This narrow region of high ionisation density at the end of the proton range is known as Bragg peak. The beam delivery techniques involve the use of passive or active beam depending on the tumour volume. Dose confirmality can be achieved using passive proton beam delivery using scattering and apertures (*S. Bhatnagar et.al*. *2012*) [4] while in active scanning technique, the whole tumour volume can be scanned using a narrow pencil beam. Relative Biological Effectiveness (RBE) of proton is also slightly higher than photons due to its dose rate, fractionation and the tissues which are being irradiated. Linear Energy Transfer (LET) is produced by secondary particles which is an estimation of "dose mean linear energy" quantity. It describes the energy deposited by the beam in the medium being traversed per unit length.

Scattered radiation in therapeutic proton beams using passive scattering has been studied by several investigators. *Binns and Hough et.al. 1997 [5]* measured the secondary dose in a 200 MeV proton beam. Yan *et.al.* 2002 [6]used a 160 MeV proton beam with a passive scattering beam delivery system to measure the neutron equivalent doses of 1–15 mSv/Gy (mSv/Gy denotes equivalent dose per treatment dose). *Polf and Newhauser et.al. 2005[7]* studied the secondary neutron dose for a passive scattering delivery system and observed a decrement in neutron dose from 6.3 to 0.63 mSv/Gy on increasing distances to isocenter from 50 to 150 cm and the dose factor also gradually increased as function of range modulation. Secondary dose was measured using Monte Carlo techniques by *Agosteo et.al. (1998)[8]* for a passive beam delivery system delivering a proton beam of 65 MeV. The absorbed dose due to neutrons was in the range $3.7\times10^{-7}$ to $1.1\times10^{-4}$ Gy per treatment Gy. The computed secondary dose due to scattered photons and neutrons varied from 0.146 to $7.1\times10^{-2}$ mGy per treatment Gy as function of depths ranging from 1 to 8 cm with a distance to the field edge of 9 to 15 cm. *Roy and Sandison et.al, 2004[9]* irradiated an anthropomorphic phantom and found that the scattered neutron equivalent dose varied between 0.1 and 0.26 mSv/Gy for the passive scattering system using a beam energy of 198 MeV. Subsequently, a systematic study on scattered neutron equivalent dose using anthropomorphic phantoms was performed (*Mesoloras et al 2006*)[10]. The neutron equivalent dose decreased on increasing aperture size. In the study by *Mesoloras et.al. (2006)* neutron equivalent dose ranges within 0.03 to 0.45 mSv/Gy and 0.1 to 0.87 mSv/Gy for a small and large field edge. *Tayama et al (2006)* [11] measured neutron equivalent doses up to 2 mSv/Gy outside of the primary radiation field in a 200 MeV proton beam. Measurements were also done using anthropomorphic phantoms and microdosimetry detectors (*Wroe et al 2007*) [12]. Equivalent doses from 3.9 to 0.18 mSv/Gy were measured when moving from 2.5 cm to 60 cm distance to the field edge.

We discussed the significance of physical and biological characteristic of proton for radiation therapy. In Section 2, the detailed architecture of Geant4 and methodology of the present work are presented. In Section 3, the results and their significance for the study and its comparison with other literature will be discussed. In Section IV, is the concluding part of the present work.

## 2. Methodology

Monte Carlo simulations performed throughout this paper is done using Geant4 toolkit which has the ability to construct standalone applications. In defining and implementation of the software mechanism, all aspects of the simulation process have been included: the geometry of the system with built-in navigation, materials, fundamental particles of interest, generation of primary particle of events, tracking of particles through materials and external electromagnetic fields, physics processes governing the particle interactions, the response of sensitive detector components, generation of the event data, the storage of events and tracks, visualization of detector, particle trajectories and capture of subsequent analysis of simulation data at different levels of aspects and its enhancement *(S.Bhatnagar et.al.)*[15]. This ultimately led to a systematic modular and hierarchical structure for the toolkit which is shown in Figure 1(a):

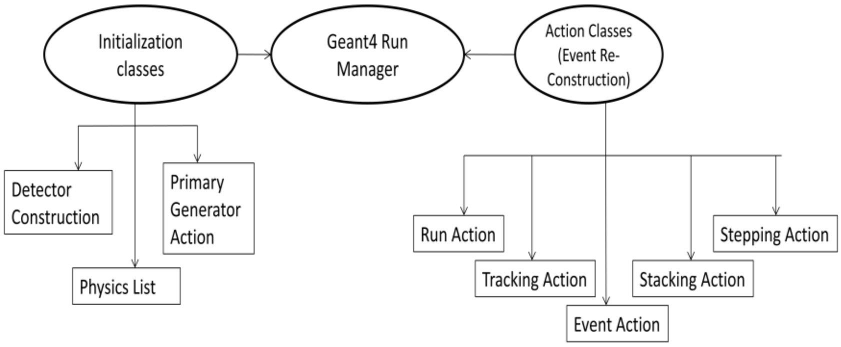


**Figure 1(a). Hierarchy System in Geant4 Toolkit**

The essential capabilities required in the Geant4 Kernel are run and event management, region dependent production thresholds and variance reduction. The configuration of a simulation setup is controlled by run manager system in Geant4. It reads the primary events which are stored in a high energy physics (HEP) standard event generator format. It also handles track vectors which can combine different sources of primary particles. There are optional helper classes which provide the information like a primary vertex, primary particle, an event and a region. The Initialization classes associated in Geant4 architecture (Figure 1(a)) customize the user requirements such as setting up the geometry, event kinematics, physics processes. The User Action classes perform the run and event processing, event verbosity which controls the order of primary and secondary particles tracking in the detector *(S. Bhatnagar et.al.)[*16]. The second significant extension of Geant4 capability is to define regions of behavior in experimental setup and different particle production threshold in each region characterized in detectors with precision capabilities (for *e.g.,*: a muon detector with an outer layer of germanium detector). This feature improves the simulation accuracy in high resolution detector saving the computing time. The user can also efficiently generate propagation of charged particles in a field associated with geometrical volume. The General Particle Source is a subsystem of Primary Generator Action class associated with architecture, shown in Figure 1(a). It has a feasible functionality to implement the particle distribution in terms of x-, y-, z- direction. An advanced technique i.e. particle tracking is developed in the Stepping Action class as a sub-system of User Action of Geant4 kernel in order to improve the performance of CPU. This technique does not depend on the particle type or on specific physics processes. The particle tracking is categorized as primary at rest, energy loss of primary particle or secondary particle production due to decay or interaction. (Jiang H *et.al.)[*17] An interface to the event generation of primary particle is defined by the event action system. It contains the list of primary vertices and particles before processing the event. The hits and digitization are further generated where the trajectories of primary particles get recorded for each event. The schematic description of Geant4 Kernel in processing event is shown in Figure 1(b).

 

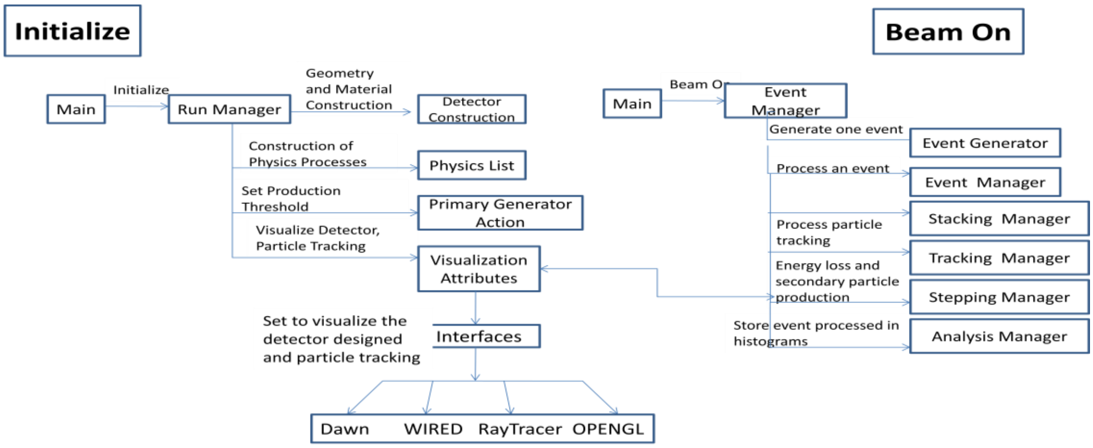


**Figure 1(b). Initialization and Event Processing in Geant4 Kernel**

The event biasing methods are used in order to facilitate the usage of variance reduction techniques which are applicable in radiation shielding studies resulting in high gain in time efficiency. It is also associated with each volume of the geometry where physics and particle tracking are defined. For each run, the whole event processing is customized by a run action class where for each begin of run, a histogram can be defined and gets stored at the end of each run. These are analyzed with help of analysis tools such as ROOT, AIDA which are interface in Analysis Manager.

Distinct human phantom organ dimensions at various ages *i.e.*, new born, 1 year, 5 year, 10 year, 15 year and Adult are considered from ORNL report [2]. Oak Ridge National Laboratory is the largest US department of energy science and energy laboratory, conducting basic and applied research to deliver transformative solutions to compelling problems in energy and security. *Fisher and Snyder et.al.* [2] developed mathematical phantom of an adult human. Here the organs are considered as the target volumes for curing tumours. The amount of absorbed dose in tumours is determined and its effect is observed on step size of the proton beam during Geant4 simulation.

The physics models used for proton therapy MC simulations are presented in this paper. The electromagnetic interactions are simulated using G4Emstandard Model which is analytical model governing the interaction of photons and charged particles of energy ≥ 1 keV. Inelastic interactions were simulated using a theory driven model based on semi-classical description of composite nucleus decay by Griffin *i.e.*, G4PreCompound Model is used for particles below 100 MeV. The G4 Binary Cascade Model which is valid in the energy range of 100 MeV – 10 GeV. It simulates the hadronic interactions as a number of binary inelastic collisions between two nucleons. Elastic interactions of hadrons were modulated using UH Elastic model. It combines the G4UHadron Elastic Process and G4 Hadron Elastic model. It incorporates the set of data for nucleon scattering. Charged particles are tracked to the end of their range in G4simulations. When a particle is defined in an interaction, the user may specify to ignore secondary production with a range less than a specified value. This is termed as range cut-off. For delta ray and bremsstrahlung production, the range cut parameter is necessary to suppress the production of huge number of soft electrons and photons. The energy suppressed via the use of a range cut is transferred to continuous process which acts along step of the parent particle. Interaction length is influenced by the choice of range cut. The energy loss process imposes a limit on the step size of the particle. A passive proton beam following a Gaussian distribution (σ = 2.5 MeV) is chosen to study the dose absorbed in target volume. The beam penetrates along the z-direction in which the phantom is placed.

Energy deposition from radiation occurs as a random number of events and the measurement of such events may lead to an increased understanding of biological effect of radiation exposure. Energy deposition in this study is typically acquired as energy spectra (f (E) vs. E). These spectra can be used to determine the absorbed dose D at the point of measurement.

$$D = \frac{\int_0^\infty f(E)dE}{\rho V}$$ Here $\rho$ is detector density and V is the volume.

A quality factor 'Q' is required for all ionising radiation which accounts for studying the impact of radiation on a tissue. This Quality factor (Q = 2) is used for protons in combination with the absorbed dose to give dose equivalent (H)

$$H = Q\,D$$

This dose equivalent is expressed in Sieverts (Sv) unit. The quality factor is designed for radiation protection purpose. It is not intended to be used for risk assessment for radiation applications. The values of Q or $W_R$ selected by ICRP based on a review of available information regarding biology radiation exposure and calculation methods.

## 3. Results and Discussion

From previous work done *(S. Bhatnagar et.al, 2014)* [1], we observed that dose distribution of proton beam in a phantom is dependent on the geometry of tumour. *Christina Zacharatou Jarlskog et.al.* [13] reported studied the equivalent dose due to secondary neutrons in pediatric and adult patients as function of patient's age, organ and field parameters. They observed the neutron dose to specific organs depend considerably on the patient's age and body stature. The younger the patient, the higher the dose is deposited due to neutrons. In this study as function of various ages, the dose distribution is not found for a new born (0 years) and 1 year. This is because of geometry factor. We observed that a finite Bragg curve can be determined from age of 5 year child whose volume is 22 $cm^3$. The dose absorbed in target volumes of phantom for various ages *i.e.*, 5, 10, 15, and an adult are shown in Figures [1-4] given below.

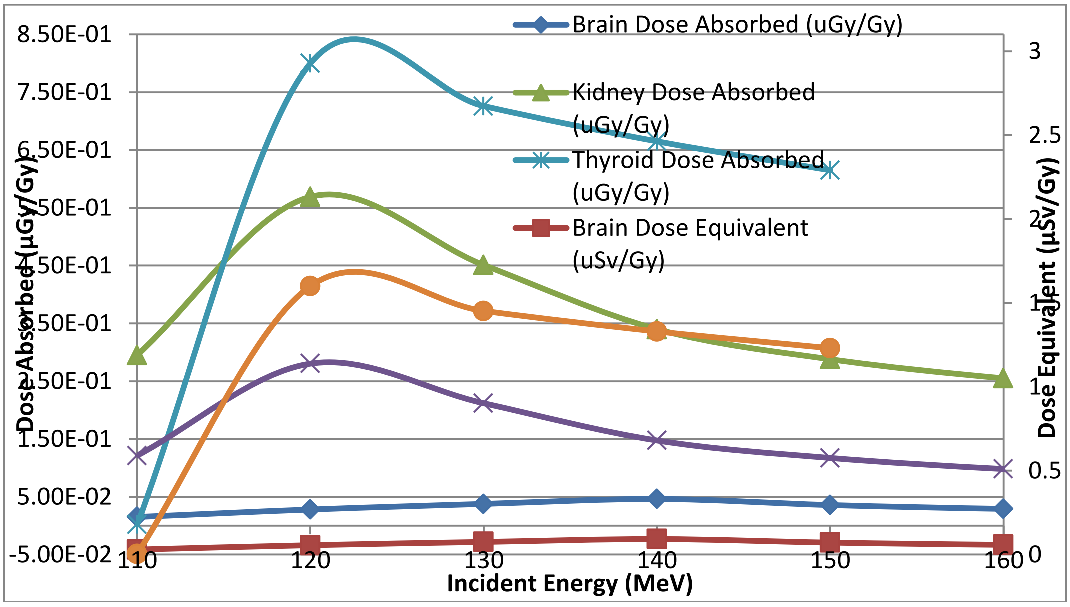


**Figure 2. Absorbed Dose, Dose Equivalent as function of Incident Energy (MeV) in 5 year Child Phantom**

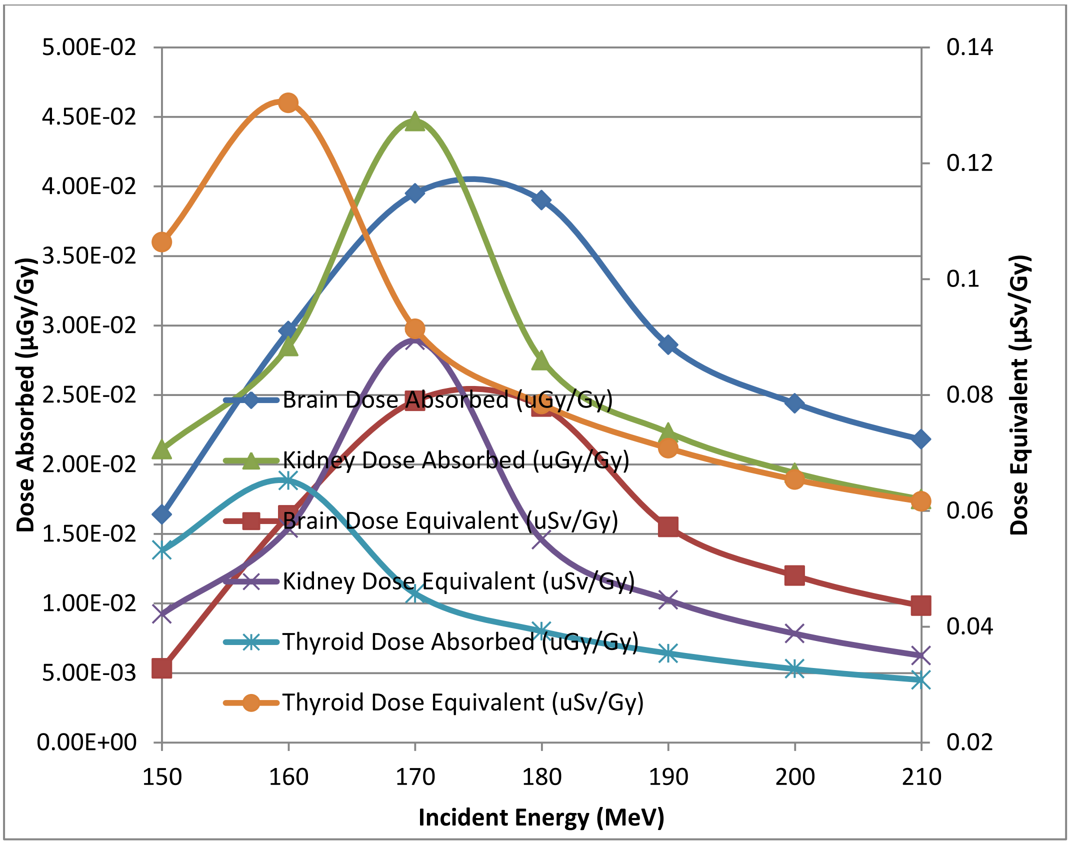


**Figure 3. Absorbed Dose, Dose Equivalent as Function of Incident Energy (MeV) in 10 year Child Phantom**

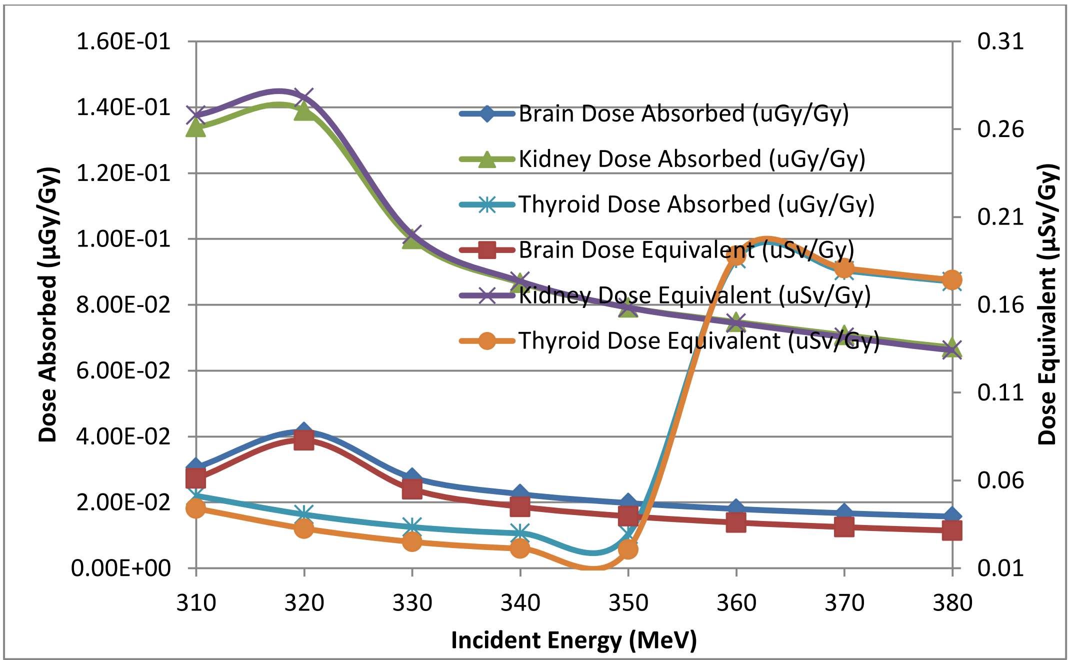


**Figure 4. Absorbed Dose, Dose Equivalent as Function of Incident Energy (MeV) in 15 year Child Phantom**

 

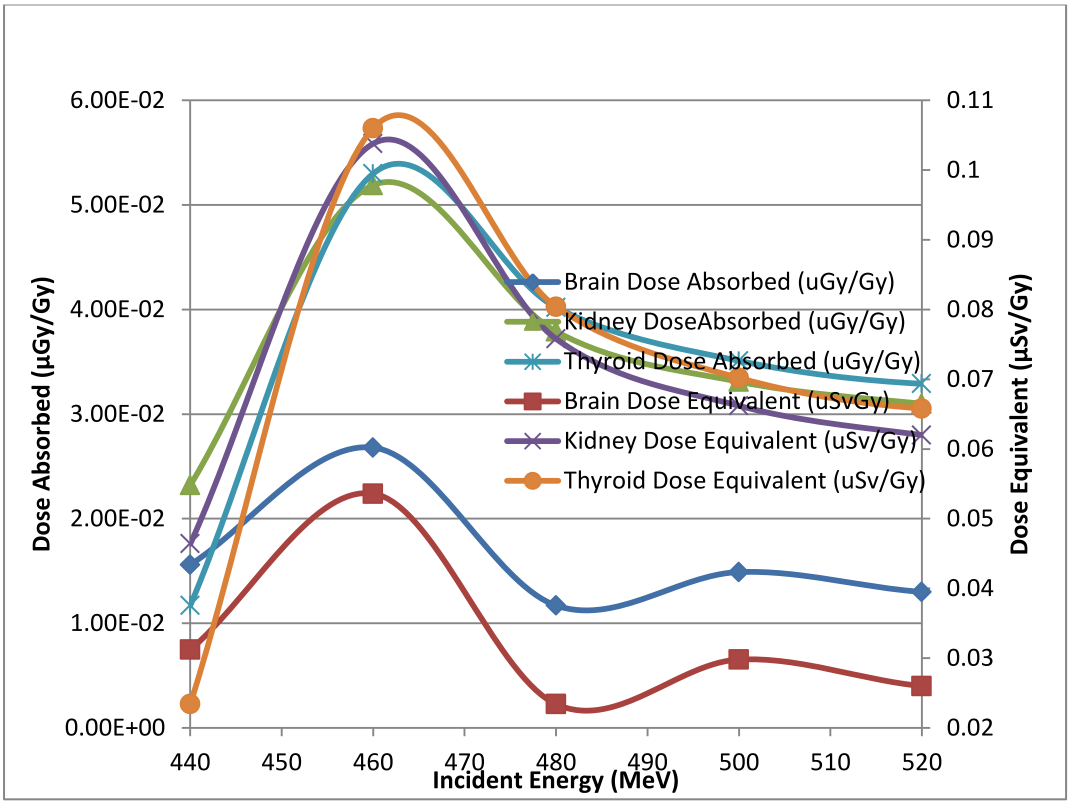


**Figure 5. Absorbed Dose, Dose Equivalent as Function of Incident Energy (MeV) in Adult Phantom**

Two factors are considered while determining the energy range *i.e.*, Dose Absorbed (Gy) and proton range traversed within the target volume of depth (cm). The dose equivalent parameter is also determined for each target volume using Quality factor of proton and dose absorbed in target volume as discussed in Section 2. The relation between absorbed dose and dose equivalent as function of depth (cm) is observed. It is shown in Figures [6 – 9]:

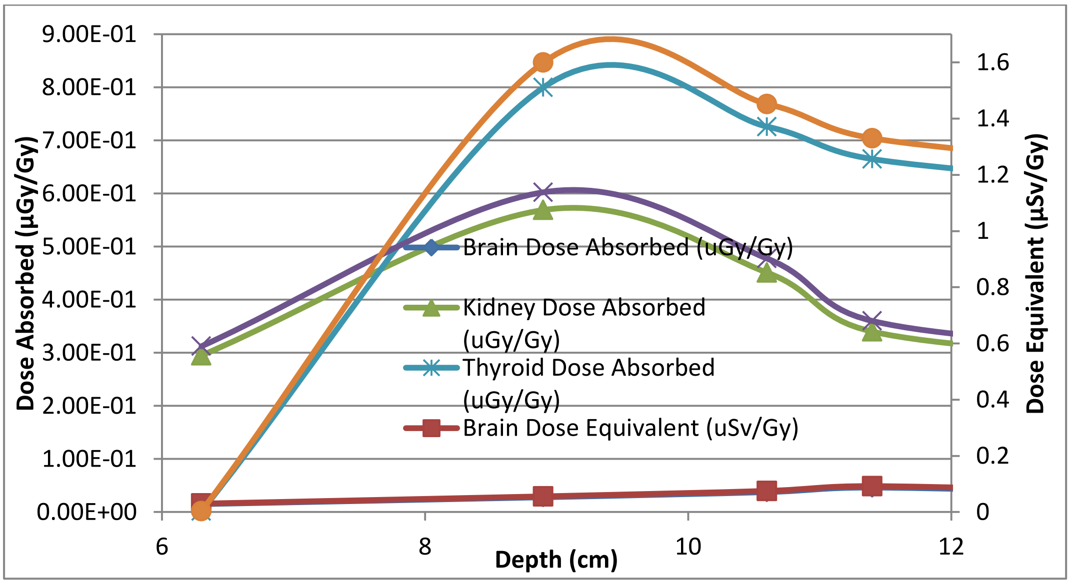


**Figure 6. Absorbed Dose, Dose Equivalent as Function of Depth (cm) in 5 year Child Phantom**

 

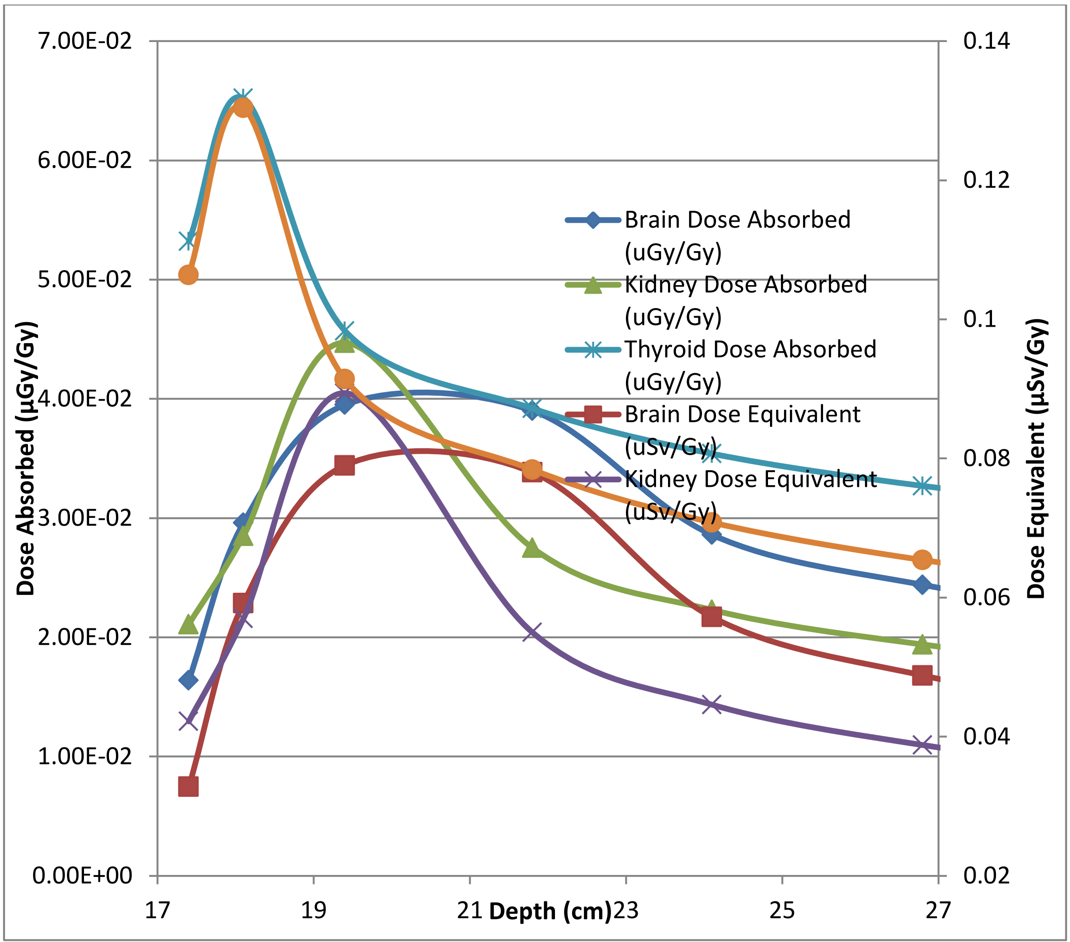


**Figure 7. Absorbed Dose, Dose Equivalent as Function of Depth (cm) in 10 year Child Phantom**

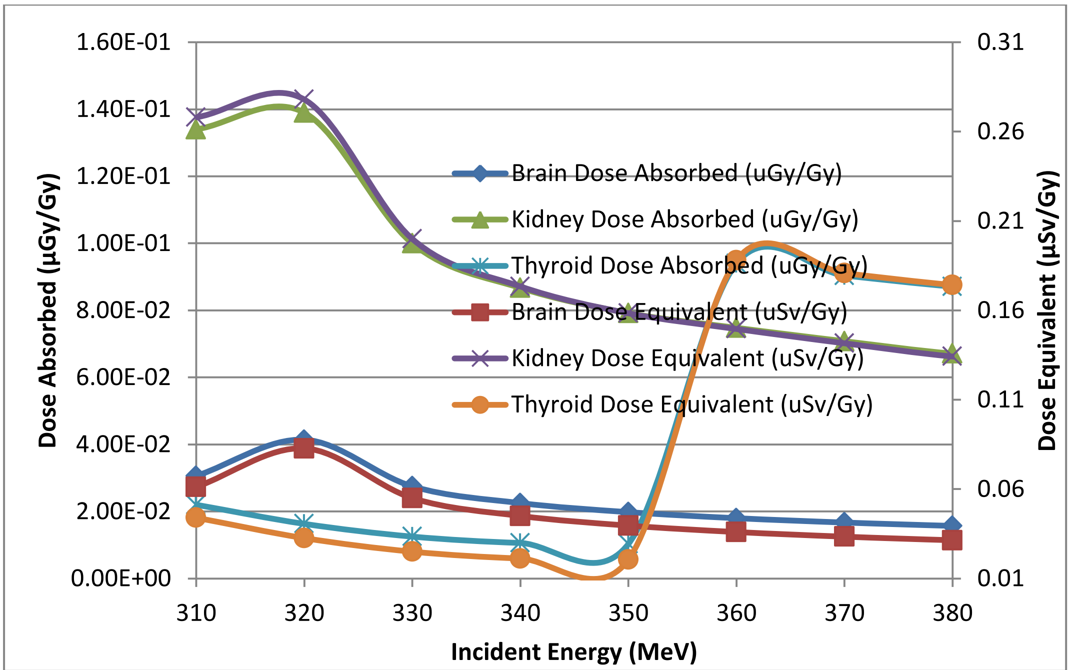


**Figure 8. Absorbed Dose, Dose Equivalent as function of Depth (cm) in 15 year Child Phantom**

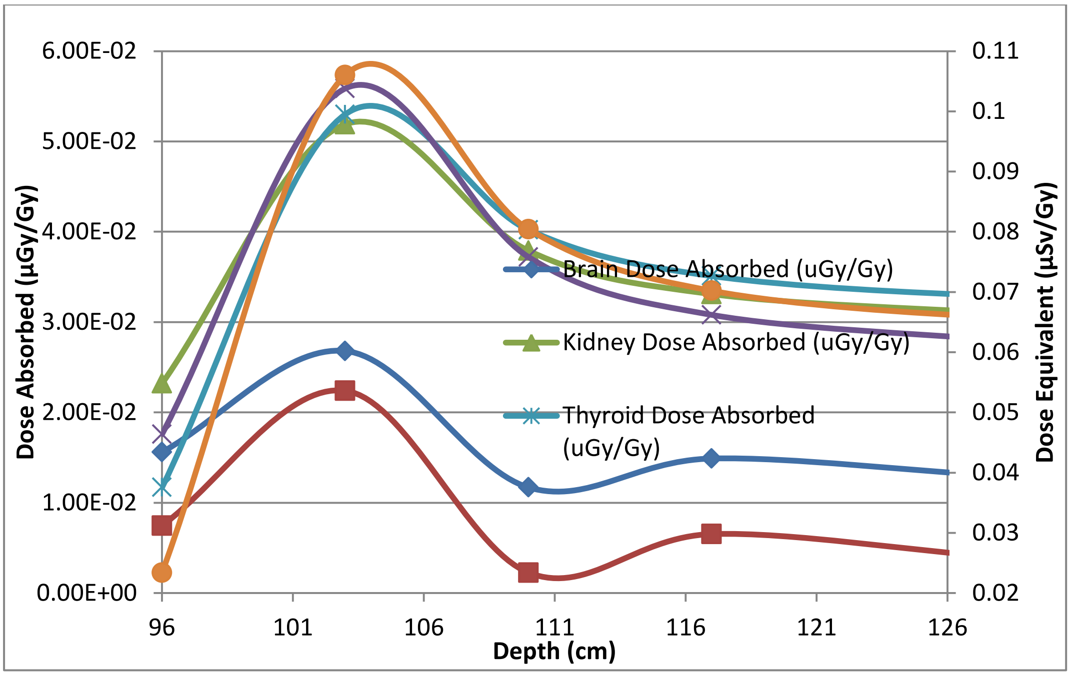


**Figure 9. Absorbed Dose, Dose Equivalent as Function of Depth (cm) in Adult Phantom**

**Table 1. Dose Equivalent for Specific Organs Obtained from Simulation**

| Phantom Age | Organs | Dose Absorbed (µGy/Gy) | Dose Equivalent (µSv/Gy) |
|---|---|---|---|
| 5 year | Brain | (0.15 – 0.46 ) | (0.30 – 0.92) |
| | Kidney | (2.32 - 5.61) | (4.64 – 11.38) |
| | Thyroid | (0.77 – 8) | (0.63 – 16) |
| 10 year | Brain | (0.13 – 0.44) | (0.32 – 0.78) |
| | Kidney | (0.71 – 2.47) | (1.28 – 2.89) |
| | Thyroid | (0.27 – 0.65) | (0.55 – 1.34) |
| 15 year | Brain | (0.11 – 0.41) | (0.23 – 0.82) |
| | Kidney | (0.58 – 1.39) | (1.18 – 2.78) |
| | Thyroid | (0.10 – 0.94) | (0.20 – 1.38) |
| Adult | Brain | (0.10 – 0.26) | (0.21 – 0.53) |
| | Kidney | (0.23 – 0.51) | (0.46 – 1.03) |
| | Thyroid | (0.11 – 0.53) | (0.23 – 1.06) |

From the above Table 1, it shows the equivalent dose deposited during proton therapy in each organ with respect to different ages of phantoms. We observed the dose deposition is dependent on the age. Patient at younger age receives dose at higher rate while it is gradually decreased in rest of the cases *i.e.*, 10 year, 15 year and Adult. In the report of *Christina Zacharatou Jarlskog et.al.*, [13], when considered the organ *i.e.*, kidney of a four year old phantom, the corresponding value ranges from (0.2 – 0.5) mSv/Gy. As in this report, they used a active scanning beam where some field parameters are considered for upstream of the aperture and spread-out Bragg peak. Due to the limitation of a experimental setup in our study, we used a passive proton beam due to which the equivalent dose deposited in our study is *i.e.*, (4.64 – 11.38) (µSv/Gy) while compared to result of *Christina Zacharatou Jarlskog et.al.*[13]. As stated in the report of *Gottschalk, Paganetti et.al, 2006* [14], passive scattered proton beams typically offer a limited set of different field sized impinging on the final aperture which may influence the yield due to its dependence on the ratio of the field size and aperture.

The effect of absorbed dose on target volume production of soft electrons and photons is observed on varying the step length of the proton. This is shown in Table 2. Here the proton beam is fixed at energy *i.e.*, 440 MeV and the dose rate was computed for Adult and it also compared among Geant4 9.3 and Gant4 9.4 versions. There is a negligible variation within the specific dose of organs as function of step length.

**Table 2. Dose Equivalent for Specific Organs Obtained from Simulation as Function of Particle Step Length**

| | Geant4.9.4 | | | | Geant4.9.3 | | |
|---|---|---|---|---|---|---|---|
| Adult | Thyroid | Kidney | Brain | Adult | Thyroid | Kidney | Brain |
| Step Length(mm) | Dose Absorbed (µGy/Gy) | | | Step Length(mm) | Dose Absorbed(µGy/Gy) | | |
| 1 | 0.11 | 0.23 | 0.159 | 1 | 0.14 | 0.215 | 0.15 |
| 2 | 0.10 | 0.21 | 0.157 | 2 | 0.10 | 0.212 | 0.15 |
| 3 | 0.09 | 0.22 | 0.156 | 3 | 0.09 | 0.213 | 0.15 |
| 4 | 0.10 | 0.21 | 0.155 | 4 | 0.09 | 0.224 | 0.15 |
| 5 | 0.10 | 0.21 | 0.154 | 5 | 0.10 | 0.216 | 0.15 |
| 6 | 0.10 | 0.21 | 0.153 | 6 | 0.10 | 0.217 | 0.15 |
| 7 | 0.10 | 0.21 | 0.153 | 7 | 0.10 | 0.21 | 0.15 |
| 8 | 0.10 | 0.20 | 0.151 | 8 | 0.10 | 0.211 | 0.15 |
| 9 | 0.09 | 0.19 | 0.147 | 9 | 0.10 | 0.209 | 0.14 |
| 10 | 0.08 | 0.20 | 0.149 | 10 | 0.08 | 0.201 | 0.14 |

## 4. Conclusion

In summary, we have shown quantitatively how organ specific proton equivalent doses for 5, 10, 15 years and an adult patients vary as a function of patient age, organ, depth and step length (a Geant4 user parameter). The dose equivalent *i.e.*, a quantity used in radiological protection to represent the stochastic health effects of low level ionizing radiation on human phantom is computed from the obtained absorbed dose and quality factor of proton beam. We observed for an organ with respect to its volume and position in the phantom, higher proton energies are required to incident on the target for curing tumours with efficient dose rate. Most importantly, our study shows that equivalent dose for specific organ depends considerably on patient age/size. The younger and smaller the patient, the higher the dose deposited via proton therapy. It needs an attention while treating pediatric patients. As per (*BEIR et.al 2006) [15]*, cancer risks also increases with decreasing patient age, extra attention must be paid to the treatment of pediatric patients. It is observed that absorbed dose in target volume of tumour is dependent on the incident energy of proton beam and geometry of target (*S. Bhatnagar et.al. 2014*) [1]. While comparing the parameter i.e. dose equivalent for specific organs as function of patient age, in case of brain it is 0.92 µGy/Gy for 5 year patient, where as the maximum dose rate decreases nearly i.e. 0.82 µGy/Gy, 0.78 µGy/Gy and 0.53 µGy/Gy for 10 year, 15 year and an adult. The range cut and step size of the particle are varied to observe the effect on dose absorption in target volume from the production of soft electrons and photons due to bremsstrahlung process which is involved in proton interaction. The accuracy of the data among the results is observed by comparing among Geant4 9.3 and 9.4 versions.

 

# References


[1] S. N. L. Sirisha and S. Bhatnagar, "Geant4 - Study of Dose Curve Parameters of Tumor in Human Tissues Using Passive Proton Beam", 2014 Sixth International Conference on Computational Intelligence and Communication Networks, IEEE Computer Society, 978-1-4799-6929-6/14 $31.00 © 2014 IEEE.

[2] M. Cristy, "Mathematical Phantoms representing children of various ages for use in Estimates of Internal Dose", Oak Ridge National laboratory, **(1980)** June.

[3] V. C. Wilson, "Proton beam irradiation in pediatric oncology: an overview", J. Ped. Hemat. Oncol, vol. 27, **(2005)**, pp. 444-448.

[4] S. N. L. Sirisha and S. Bhatnagar, "GEANT4 & GAMOS- A Particle Implementation of High Energy Simulation Toolkit to Oncology Therapy", Proceeding of the 2014 IEEE Students' Technology Symposium, 978-1-4799-2608-4/14/ 2014 IEEE.

[5] P. J. Binns and J. H. Hough, "Secondary dose exposures during 200 MeV proton therapy", Radiat. Prot. Dosim, vol. 70, **(1997)**, pp. 441-444.

[6] X. Yan, "Measurement of neutron dose equivalent to proton therapy patients outside of the proton radiation field", Nucl. Instrum. Methds. Phys. Res. A, vol. 476, **(2002)**, pp. 429-434.

[7] J. C. Polf, "Calculations of neutron dose equivalent exposures from range-modulated proton therapy beams", Phys. Med. Biol., vol. 50, **(2005)**, pp. 3859-3873.

[8] S. Agosteo, C. Birattari, M. Caravaggio, M. Silari and G. Tosi, "Secondary neutron and photon dose in proton therapy", Radiother. Oncol., [PubMed: 9925249], **(1998)**, pp. 48:293-305.

[9] S. C. Roy and G. A. Sandison, "Scattered neutron dose equivalent to a fetus from proton therapy of the mother", Radiat. Phys. Chem., vol. 71, **(2004)**, pp. 997-998.

[10] G. Mesoloras, "Neutron Scattered Dose equivalent to a fetus for proton radiotherapy of the mother", Med. Phys., vol. 33, **(2006)**, pp. 2479-2490.

[11] R. Tayama, Y. Fujita, M. Tadokoro, H. Fujimaki, T. Sakae and T. Terunuma, "Measurement of neutron dose distribution for a passive scattering nozzle at the Proton Medical Research Centre", Nucl. Instr. Methods., Phys. Res. A, vol. 564, **(2006)**, pp. 532-536.

[12] A. Wroe, "Out-of-field dose equivalents delivered by proton therapy of prostate cancer". Med. Phys., vol. 34, **(2007)**, pp. 3449-3456.

[13] C. Zacharatou Jarlskog, "Assessment of organ specific neutron equivalent doses in proton therapy using computational whole body age dependent voxel phantoms", Phys. Med Biol., vol. 53, no. 3, **(2008)** February 7, pp. 693-717.

[14] B. Gottschalk and H. Paganetti, "Neutron dose in scattered and scanned proton beams: in regard to Eric J. Hall (Int. J Radiat Oncol Biol Phys 2006; 65: 1-7)", International Journal of Radiat. Oncol. Biol Phys., vol. 66, **(2006)**, pp. 1594.

[15] S. Sathiraju Naga lakshmi and S. Bhatnagar, "Stopping Power of Proton Beam in Water Phantom: A Simulational Study", Recent Advancements in System Modelling Applications, Lecture Notes in Electrical Engineering 188, DOI: 10.1007/978-81-322-1035-1_8, Springer India, **(2013)**.

[16] V. Yadav, S. N. L. Sirisha and S. Bhatnagar, "Study for Stopping Power of Proton in Different materials – A Geant4 Simulation", Proceedings of the DAE Symp. on Nucl. Phys., vol. 57, **(2012)**.

[17] H. Jiang, B. Wang, X .G Xu, H. D. Suit and H. Paganetti, "Simulation of Organ Specific Patient Effective Dose Due to Secondary Neutrons in Proton Radiation Treatment", Phys. Med. Biol., [PubMed: 16148397], vol. 50, **(2005)**, pp. 4337-4353.

[18] S. J. Dowdell, "Pencil Beam scanning proton therapy: the significance of secondary particles", **(2011)**.